

# Studies on a Pressurized Type Under-floor Air Conditioning System (Analysis of Governing Factors for Uniform Air Velocity Profile)

Atsushi TAKAHASHI and Chol Num KONG

Takasago Thermal Engineering Co., LTD

R & D Center

3150, Iiyama, Atsugi, Kanagawa, JAPAN

## Summary

Recently, a lower type free-access floor system which realizes improved ease of walking and less sense of confinement has been attracting attention. However, it is known that the lower the design of the air supply chamber, the larger the non-uniformity of the diffuser air velocity profile and the greater the deterioration in room temperature distribution. In this paper, an analytical model is proposed for predicting the non-uniformity of diffuser air velocity at the design stage. The validity of the analytical model was confirmed by the good coincidence of results obtained in scale model experiments. It was found that the limit of the floor height at which a uniform diffuser air velocity is obtained was 50 mm. Moreover, a relation was found whereby the inverse of coefficient of resistance at a diffuser up to a value of 1 is proportional to the maximum non-uniformity. This indicates the possibility that design work aimed at constructing a pressurized type under-floor air conditioning system with a uniform air velocity profile from diffusers may be readily performed from parameters of the coefficient of resistance at a diffuser by utilizing this relation.

## 1. Introduction

The rapid spread of information processing equipment has occasioned the adoption of free-access floor system in offices, in which can be housed power lines, communication cables and other items, and which lends itself to changes in layout. Recently, there has been much interest in lower type free-access floor systems which provide improved comfort when walking and alleviate the sense of confinement which is a problem with other systems. If the space in lower systems could be used to house air supply chambers for air conditioning system, the construction costs required for an under-floor air conditioning system could be reduced. However, the lower the floor, the less uniform the air velocity profile from diffusers. And, it is known that in a pressurized type under-floor air conditioning system, excessive pressurization of air supply chambers can cause air leakage, so that the thermal environment of the room is degraded as a result.

There have been numerous reports of scale model experiments on pressurized type under-floor air conditioning systems and measurements of thermal environments. However, there have been extremely few studies analysing the air velocity profile. In this paper, we propose a model which can be used to analyze the non-uniformity in the air velocity profile, and after verifying the

validity of the model through scale model experiments, we studied the floor height lower limit the limits to establishment of analytical equations. In addition, the sensitivity of factors governing non-uniformity in diffuser air velocity was analyzed, and a method for adjustment to make velocity profiles more uniform, as well as a simple design technique to determine the diameter of air diffuser outlets and the height of air supply chambers, were proposed.

## 2. Construction of an Analytical Model

The assumptions for the purpose of constructing an analytical model were as follows;

Assumption (1) : The pressure within the chamber is higher than the air pressure in the room (condition of continuity)

Assumption (2) : An equal diffused air velocity is obtained at all diffuser outlets. (continuum uniform division branch model)

Assumption (3) : The diffused air velocity is proportional to the 1/2 power of the pressure difference between the chamber and the room. (turbulent flow model)

Assumption (4) : The air velocity in the chamber is distributed only in the length direction. (one-dimensional model)

Assumption (5) : A state of thermal uniformity obtains within the chamber. (isothermal model)

### 2.1 Mass Balance

Physical parameters such as the height of the chamber and the diameter of diffuser outlet, air flow and pressure loss are indicated in Figure 1. From the mass balance, we obtain the following relations;

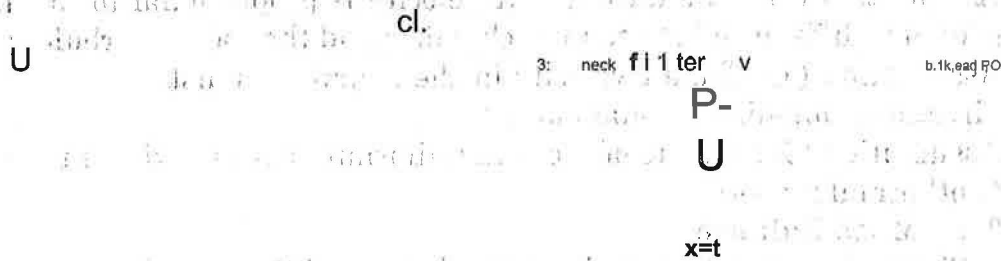


Fig. 1 Analytical model for supply chamber and diffusers.

Diffuser aperture area:	$1$	$s = RK \cdot (7r \cdot d^2 / 4) \cdot M \cdot N$	----
Diffuser aperture ratio:	$K$	$7 - s / 1 (L \cdot W)$	----

Ratio of air path cross-section to floor area:	$8$	$(D \cdot W) / (L \cdot W)$	----
Neck air velocity of chamber:	$U$	$(Q / 3600) / 6$	----
Diffuser air velocity:	$v$	$\sqrt{1 - U^2} / K$	(51)

### 2.2 Momentum Balance

Taking the coordinate origin at the bulkhead, we use Equation (6) to approximate the air velocity at position  $x$  in the chamber length direction.

validity of the model through scale model experiments, we studied the floor lower limit and the limits to establishment of analytical equations. In addition, the sensitivity of factors governing non-uniformity in diffuser air velocity was analyzed, and a method for adjustment to make air velocity profiles more uniform as well as a simple design technique to determine the diameter of air diffusers and the height of air supply chambers, were proposed.

## 2. Construction of an Analytical Model

The assumptions for the purpose of constructing an analytical model are as follows;

Assumption (1) : The pressure within the chamber is higher than the air pressure in the room. (condition of continuity)

Assumption (2) : An equal diffused air velocity is obtained at all diffuser outlets (continuous uniform division branch model)<sup>2)</sup>

Assumption (3) : The diffused air velocity is proportional to the 1/2 power of the pressure difference between the chamber and the room. (turbulent flow model)

Assumption (4) : The air velocity in the chamber is distributed only in the longitudinal direction. (one-dimensional model)

Assumption (5) : A state of thermal uniformity obtains within the chamber. (isothermal model)

### 2.1 Mass Balance

Physical parameters such as the height of the chamber and the diameter of the diffuser outlet, air flow and pressure loss are indicated in Figure 1. From mass balance, we obtain the following relations;

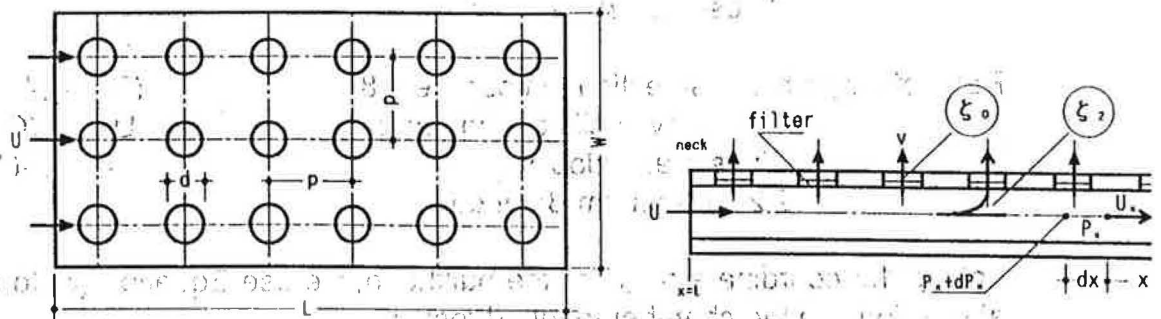


Fig. 1 Analytical model for supply chamber and diffusers.

Diffuser aperture area:  $\Sigma s = RK \cdot (\pi \cdot d^2 / 4) \cdot M \cdot N$  --

Diffuser aperture ratio:  $\kappa = \Sigma s / (L \cdot W)$  --

Ratio of air path cross-section to floor area:  $\beta = (D \cdot W) / (L \cdot W)$  --

Neck air velocity of chamber:  $U = (Q / 3600) / \beta$  --

Diffuser air velocity:  $v = \beta \cdot U / \kappa$  --

### 2.2 Momentum Balance

Taking the coordinate origin at the bulkhead, we use Equation (1) to approximate the air velocity at position x in the chamber length direction.

$$U_x = x \cdot U/L \quad \text{----- (6)}$$

The fluid momentum in the interval from  $x$  to  $x+dx$  is as in Equation (7).  
 $(R+dp_x) + (P - 12) \cdot (U_x + dU_x)^2 = R_x + (p/2) \cdot U_x^2 + (p/2) \cdot A \cdot (dx)^{-1} DE \cdot U_x^2$   
 + (main stream branch loss) ----- (1)

The equivalent diameter of chamber (3) and tube friction coefficient, are computed using Equation and Equation (9). Here  $E$  and  $Re$  are the relative roughness and the Reynolds number, respectively.

$$\frac{DE}{A} = \frac{1.3 \cdot [(W/D)F] \cdot (W+D)^{2.10.12.7}}{0.0055 \cdot [1 + (20000 \cdot \text{-----} (9))]} \quad \text{----- (8)}$$

The momentum balance between the origin and position  $x$  is obtained by integrating Equation (7) showed as Equation (10).

$$f \, dp = (p_x)^2 - (U/L)^2 \int_A X^2 \cdot Di^{-2} x \, dx + (\text{sum of main stream branch losses}) \quad \text{----- (10)}$$

In Equation (5), the sum of the main stream branch losses can be approximated by zero. Hence pressure difference within the chamber corresponding to the position of the  $n$ th diffuser outlet is given Equation (11).

$$P_n - P_o = [A \cdot n \cdot p_x^{-1} (3 \cdot Di_x)^{-1}] \cdot (p_x)^2 \cdot (n \cdot p/L)^2 \cdot U^2 \quad \text{----- (11)}$$

On the other hand, the position of appearance of the minimum pressure is obtained from the condition  $dp_x/dx = 0$ , and becomes  $X_{i,i} = n \cdot p = 2 \cdot D_{E,i}/A$ . When  $0 < X_{i,i} < L$ , the position of minimum pressure occurs within the chamber; if we suppose that the  $i$ th diffuser outlet corresponds to the position occurrence of the **minimum** pressure, then the pressure difference within the **chamber** corresponding to the position of the  $i$ th outlet is as given by Equation (12).

91

$$P_{i,i} - P_o = [A \cdot m \cdot p_x^{-1} (3 \cdot DF_{i,i})^{-1}] \cdot (p_{i,i})^2 \cdot (m \cdot p_x/L)^2 \cdot U^2 \quad \text{----- (12)}$$

The interval from the coordinate origin to the first diffuser outlet can be approximately given  $p$  therefore, the necessary pressure difference between the bulkhead and the room to obtain a desired diffuser air velocity is given by Equation (13).

$$p_o - p_i = (1 + (p_o/HP)^2) \cdot U^2 + [A \cdot p_x^{-1} DE_1 (P @, 2) - (p_x)^2, L]^2 \cdot U^2 + P_f(V) \quad \text{----- (13)}$$

At the position of the  $i$ th diffuser outlet, Assumption (1) for construction of an analytical model obtained the necessary pressure difference between the  $n$ th

$$U_x = x \cdot U / L \quad \text{-----}$$

The fluid momentum in the interval from  $x$  to  $x+dx$  is as in Equation (7).

$$(P_x + dP_x) + (\rho / 2) \cdot (U_x + dU_x)^2 = P_x + (\rho / 2) \cdot U_x^2 + (\rho / 2) \cdot \lambda \cdot (dx / D_E) \cdot U_x^2 + \text{(main stream branch loss)} \quad \text{-----}$$

The equivalent diameter of chamber<sup>3)</sup> and tube friction coefficient computed using Equation (8) and Equation (9). Here  $\epsilon$  and  $Re$  are the roughness and the Reynolds number, respectively.

$$D_E = 1.3 \cdot [(W \cdot D)^5 / (W + D)^2]^{0.125} \quad \text{-----}$$

$$\lambda = 0.0055 \cdot [1 + (20000 \cdot \epsilon / D_E + 106 / Re)^{1/3}] \quad \text{-----}$$

The momentum balance between the origin and position  $x$  is obtained by integrating Equation (7) and showed as Equation (10).

$$\int dP_x = (\rho / 2) \cdot (U / L)^2 \int [\lambda \cdot x^2 / D_E - 2x] dx + \text{(sum of main stream branch losses)} \quad \text{-----}$$

In Equation (5), the sum of the main stream branch losses can be approximated by zero.<sup>2)</sup> Hence the pressure difference within the chamber corresponding to the position of the  $n$ th diffuser outlet is given by Equation (11).

$$P_n - P_0 = [\lambda \cdot n \cdot p / (3 \cdot D_E) - 1] \cdot (\rho / 2) \cdot (n \cdot p / L)^2 \cdot U^2 \quad \text{-----}$$

On the other hand, the position of appearance of the minimum pressure is obtained from the condition  $dP_n / dn = 0$ , and becomes  $X_{min} = m \cdot p = 2 \cdot D$ . When  $0 < X_{min} < L$ , the position of minimum pressure occurs within the chamber. We suppose that the  $m$ th diffuser outlet corresponds to the position of occurrence of the minimum pressure, then the pressure difference within the chamber corresponding to the position of the  $m$ th outlet is as given by Equation (12).

$$P_m - P_0 = [\lambda \cdot m \cdot p / (3 \cdot D_E) - 1] \cdot (\rho / 2) \cdot (m \cdot p / L)^2 \cdot U^2 \quad \text{-----}$$

The interval from the coordinate origin to the first diffuser outlet can be approximately given  $p/2$ , therefore, the necessary pressure difference between the bulkhead and the room to obtain a desired diffuser air velocity is given by Equation (13).

$$P_0 - P_r = (1 + \zeta_0) \cdot (\rho / 2) \cdot v^2 + [\zeta_2 + \lambda \cdot p / D_E] \cdot (\rho / 2) \cdot (p / 2 / L)^2 \cdot U^2 + P_f(v) \quad \text{-----}$$

At the position of the  $m$ th diffuser outlet, Assumption (1) for construction of an analytical model obtains, and the necessary pressure difference between the

diffuser outlet and the room to obtain a desired air flow velocity is as in Equation (14).

$$P_n - P_r = (1 + \frac{C_d^2}{2}) \cdot \frac{\rho \cdot v_n^2}{2} + \left[ \frac{1}{2} + \frac{A_n \cdot \rho \cdot v_n^2}{DE} - 11(P_n - P_r) \right] \cdot (m \cdot \rho \cdot v_n^2) \quad (14)$$

Depending on the position of occurrence of the minimum pressure, the following two types of distribution of pressure differences between diffusers and a room may appear. Pressure differences between the nth diffuser outlet and the room when  $0 < X_i < L$  is of the form shown at the top in Figure 2, and given by the following equation.

$$(P_n - P_r) = (R' - P_o) + W(-P_n) \quad (15)$$

On the other hand, the pressure difference between the nth diffuser outlet and the room when  $0 < X_i < L$  is as shown at the bottom of Figure 2, and given by Equation (16).

$$(P_n - P_r) = (P_n - p_o) + (P_n - P'') + (P_{n+1} - P_n) \quad (16)$$

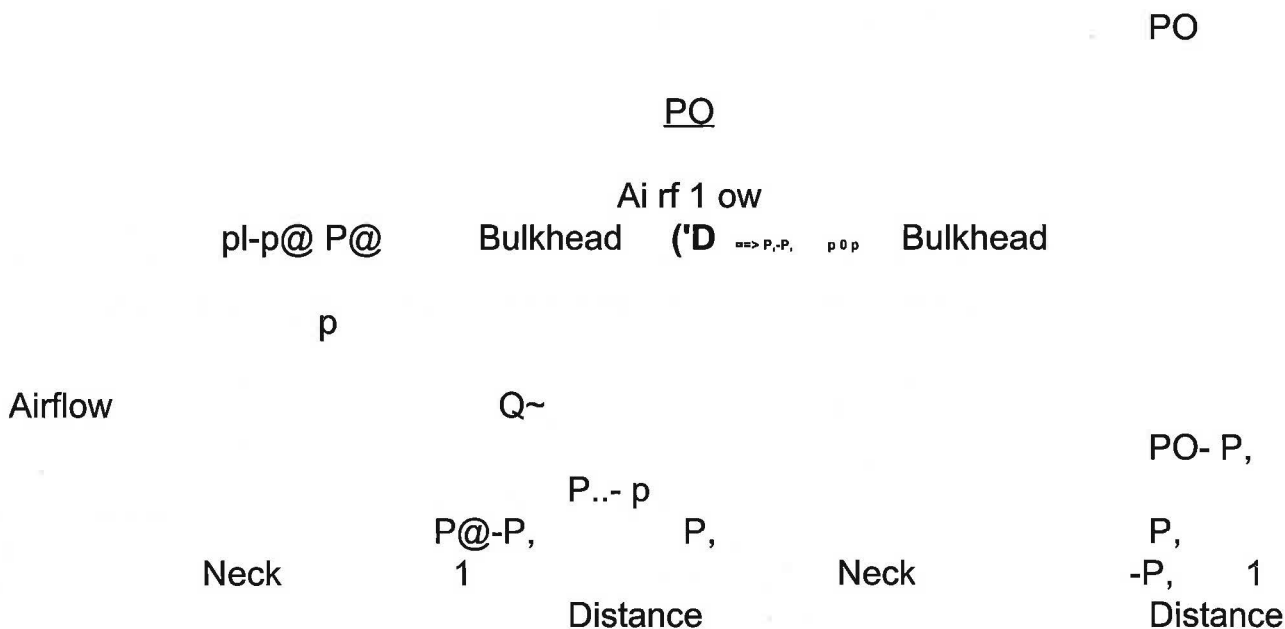


Fig. 2 Two typical necessary pressure difference profiles between diffusers and a room.

The diffuser air velocity at the nth position may be computed using the following equation applying Assumption (3), given the pressure difference between the nth diffuser and the room as computed using analytical models.

$$v_n = C_d \cdot \sqrt{2 \cdot (P_n - P_r) / \rho} \quad (17)$$

In order for the continuity condition to hold, the air velocity at each diffuser must coincide with the average of the diffuser air velocity as determined from the analytical model.

The constant of proportionality  $C()$  is chosen such that the average value of the computed air velocities coincides with the air velocities at each diffuser obtained from the supply flow.

As the outlet orifice loss coefficient, the value 2.4, equal to the average for the

diffuser outlet and the room to obtain a desired air flow velocity is as in Eq (14).

$$P_m - P_r = (1 + \zeta_0) \cdot (\rho / 2) \cdot v^2 + [\zeta_2 + \lambda \cdot p / D_E - 1] \cdot (\rho / 2) \cdot (m \cdot p / L)^2 \cdot U^2 + P_r(v) \quad \text{-----}$$

Depending on the position of occurrence of the minimum pressure, the following two types of distribution of pressure differences between diffusers and a room appear. Pressure differences between the  $n$ th diffuser outlet and the room  $X_{\min} \geq L$  is of the form shown at the top in Figure 2, and given by the following equation.

$$(P_n - P_r) = (P_n - P_0) + (P_0 - P_r) \quad \text{-----}$$

On the other hand, the pressure difference between the  $n$ th diffuser outlet and the room, when  $0 < X_{\min} < L$  is as shown at the bottom of Figure 2, and given by Equation (16).

$$(P_n - P_r) = (P_n - P_0) + (P_0 - P_m) + (P_m - P_r) \quad \text{-----}$$

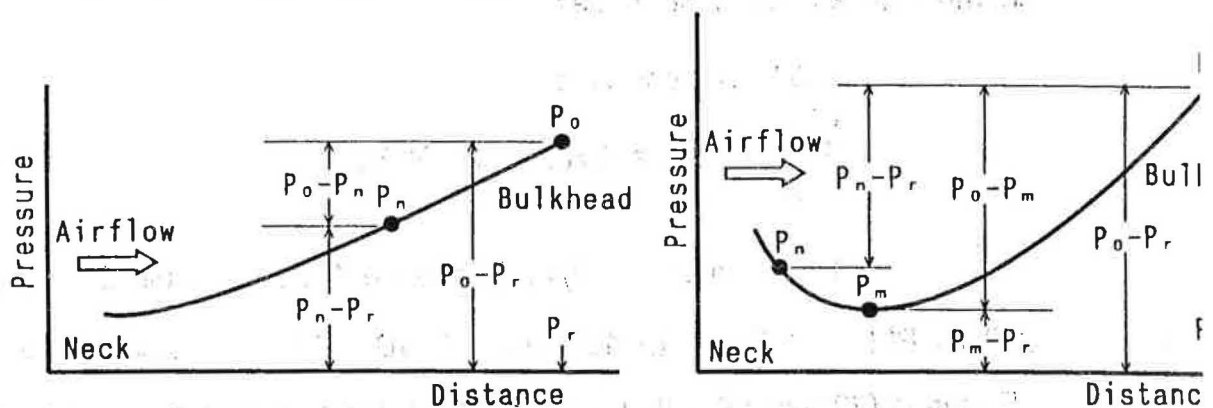


Fig. 2 Two typical necessary pressure difference profiles between diffusers and a room.

The diffuser air velocity at the  $n$ th position may be computed using the following equation applying Assumption (3), given the pressure difference between the diffuser and the room as computed using analytical models.

$$v_n = C_D \cdot \{2 \cdot (P_n - P_r) / \rho\}^{1/2} \quad \text{-----}$$

In order for the continuity condition to hold, the air velocity at each diffuser must coincide with the average of the diffuser air velocity as determined from analytical model  $v_n$ . The constant of proportionality  $C_D$  is chosen such that the average value of the computed air velocities coincides with the air velocity at each diffuser obtained from the supply air flow.

As the outlet orifice loss coefficient, the value 2.4, equal to the average for



path based on the resistance of the flow passing through the outlet, was employed.,5) As branch loss coefficient, the value 1.1, equal to the average for the path based on the branch I for a uniform-flow tube, was employed. The air velocity per diffuser outlet obtained from supply air flow is equivalent to the design air flow assuming that the air flow is divided equally among all diffusers. This air velocity is denoted by  $v(\text{design})$ ; using the design air flow reference, the absolute value of the deviation in the diffuser air velocity is defined to be the non-uniformity in the diffuser air velocity. Its maximum value is further defined to be the maximum non-uniformity.

$$NU = \frac{1}{n} \sum_{i=1}^n \frac{|v_i - v(\text{design})|}{v(\text{design})} \cdot 100 \quad \text{----- (18)}$$

The irregularity in the diffuser air velocity was adjusted by adding filters of equal resistance uniformly to all diffusers.

The filter resistance is expressed as a function of the diffuser air velocity. Here, for convenience in using  $P_f$  to denote the filter resistance at a

we consider the diffuser air velocity  $v_0 = 1$  [m/s]. Hence the filter resistance for an arbitrary air velocity is as follows;

$$P_f(v) = P_{f0} \cdot (v/v_0)^2 \quad \text{----- (19)}$$

### 2.3 Range of Validity of Analytical Model

Equation (20) and Equation (21) express the conditions of mass and momentum balance at chamber neck and diffuser outlets.

$$\rho D W U = \rho v T E_s \quad \text{----- (20)}$$

$$P_i + (\rho/2) U^2 = P_o + (\rho/2) V^2 + P_f(V) \quad \text{----- (21)}$$

From Equation (20) and Equation (21), we obtain Equation (22).

$$\frac{P_i + P_f(v) - P_o}{\rho} = (\frac{D W U}{T E_s})^2 \cdot \frac{1}{2} - (\frac{D W U}{T E_s})^2 \cdot \frac{1}{2} \cdot (\frac{V}{U})^2 \quad \text{----- (22)}$$

Equation (22) indicates that the sign of the pressure difference between the chamber neck and diffuser outlets is reversed at  $(\frac{D W U}{T E_s}) = 1$ . The condition for air to flow from the neck to diffuser outlets is  $P_i + P_f(v) > P_o$ . The condition  $(\frac{D W U}{T E_s}) > 1$  does not satisfy Assumption (1), and so the condition that the ratio of the air path cross-sectional area at the neck to the total area of the diffuser outlets be greater than unity must be met for the analytical model to obtain.

### 3. Analysis of Non-uniformity in Air Flow Velocities

We define the unit air volume as the air flow required to accommodate the air conditioning load per unit floor area. Diffuser air flow velocities were analyzed

path based on the resistance of the flow passing through the outlet employed.<sup>5)</sup> As the branch loss coefficient, the value 1.1, equal to the average the path based on the branch loss for a uniform-flow tube, was employed.<sup>6)</sup> The air velocity per diffuser outlet obtained from the supply air flow is equivalent to the design air flow assuming that the air flow is divided equally among the diffusers. This air velocity is denoted by  $v(\text{design})$ ; using the design air flow as a reference, the absolute value of the deviation in the diffuser air velocity is denoted by  $\delta v$  to be the non-uniformity in the diffuser air velocity. Its maximum value is further defined to be the maximum non-uniformity.

$$NU_n = \frac{|v_n - v(\text{design})|}{v(\text{design})} \cdot 100 \quad \text{-----}$$

The irregularity in the diffuser air velocity was adjusted by adding filter resistance uniformly to all diffusers.

The filter resistance is expressed as a function of the diffuser air velocity. For design convenience in using  $P_{r0}$  to denote the filter resistance at a diffuser air velocity  $v_0 = 1$  [m/s]. Hence the filter resistance for an arbitrary diffuser air velocity is as follows;

$$P_r(v) = P_{r0} \cdot (v/v_0)^2 \quad \text{-----}$$

### 2.3 Range of Validity of Analytical Model

Equation (20) and Equation (21) express the conditions of mass and momentum balance at the chamber neck and diffuser outlets.

$$\begin{aligned} \rho \cdot D \cdot W \cdot U &= \rho \cdot v \cdot \Sigma s & \text{-----} \\ P_1 + (\rho/2) \cdot U^2 &= P_n + (\rho/2) \cdot v^2 + P_r(v) & \text{-----} \end{aligned}$$

From Equation (20) and Equation (21), we obtain Equation (22).

$$\begin{aligned} \{P_n + P_r(v) - P_1\} &= (\rho/2) \cdot U^2 \cdot \{1 - (D \cdot W / \Sigma s)^2\} \\ &= (\rho/2) \cdot U^2 \cdot \{1 - (\beta / \kappa)^2\} & \text{-----} \end{aligned}$$

Equation (22) indicates that the sign of the pressure difference between the chamber neck and diffuser outlets is reversed at  $(D \cdot W / \Sigma s) = 1$ . The condition for air to flow from the neck toward diffuser outlets is  $P_1 \geq \{P_n + P_r(v)\}$ . The condition  $(D \cdot W / \Sigma s) \leq 1$  does not satisfy Assumption (1), and so the condition that the ratio of the air path cross-sectional area at the neck to the total area of the diffuser outlets be greater than unity must be met for the analytical model to obtain.

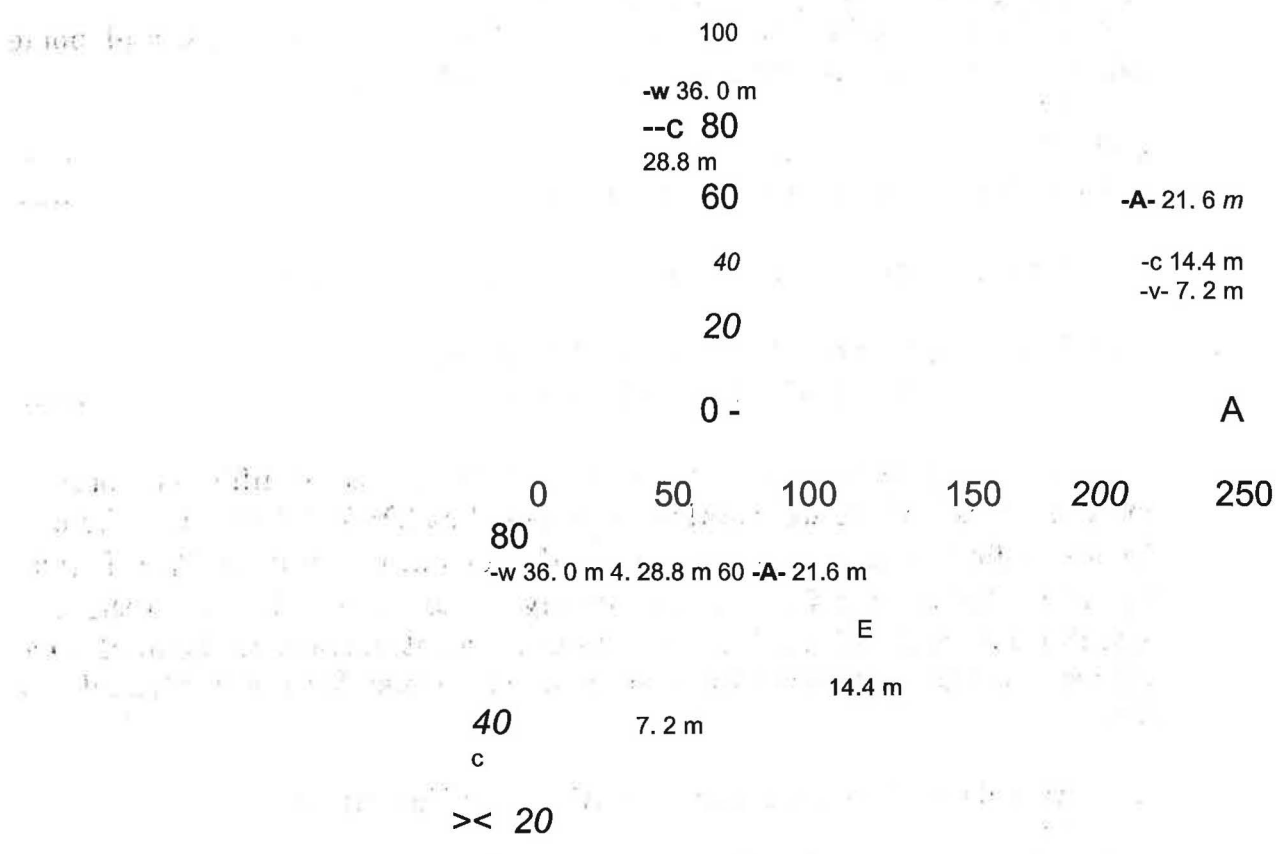
### 3. Analysis of Non-uniformity in Air Flow Velocities

We define the unit air volume as the air flow required to accommodate the conditioning load per unit floor area. Diffuser air flow velocities were ana-

for the range of values appearing in Table 1.

Table 1 . Dimensions and the given range of physical parameters.

Physical Parameter	Symbol	Unit	Quantity		
unit supplied air volume	Q	m <sup>3</sup> /m <sup>2</sup> .h	30	40	50
width of chamber	W	m	4.8		
height of chamber	D	m	0.05	-	0.30
length of chamber	l	m	7.20	-	36.0
effective opening ratio	RK		0.4		
pitch of diffuser	p	m	1.2		
diameter of diffuser	d	m	0.10	-	0.30
density of air	$\rho$	kg/m <sup>3</sup>	1.217 at 17T		
outlet loss coefficient	0		2.4		
branch loss coefficient					



0

0 50 100 150 200 250  
D mm

Fig. 3 Relation between  $NU_{si}$ , and  $X_{min}$  at various chamber heights. ( $d = 200 = 30$ )

In general, the effective aperture of a diffuser outlet varies with the outlet diameter, but here take all apertures to be 0.4. In consideration of the

'bility of rupture of the caulking in floor seams, the upper limit to chamber possi 1 1

pressurization was set at 50 Pa.8)

Figure 3 shows an example of analysis of the maximum non-uniformity resulting when the diffuser o resistance is not adjusted using filters. When  $X_{in} > L$ , the dynamic pressure near the neck area is h and diffuser air flows are lower than the design values. As a result the maximum non-uniformity in

for the range of values appearing in Table 1.

Table 1. Dimensions and the given range of physical parameters.

Physical Parameter	Symbol	Unit	Quantity
unit supplied air volume	Q	m <sup>3</sup> /m <sup>2</sup> ·h	30 40 50
width of chamber	W	m	4.8
height of chamber	D	m	0.05 ~ 0.30
length of chamber	L	m	7.20 ~ 36.0
effective opening ratio	RK	-	0.4
pitch of diffuser	p	m	1.2
diameter of diffuser	d	m	0.10 ~ 0.30
density of air	ρ	kg/m <sup>3</sup>	1.217 at 17°C
outlet loss coefficient	ζ <sub>o</sub>	-	2.4
branch loss coefficient	ζ <sub>z</sub>	-	1.1

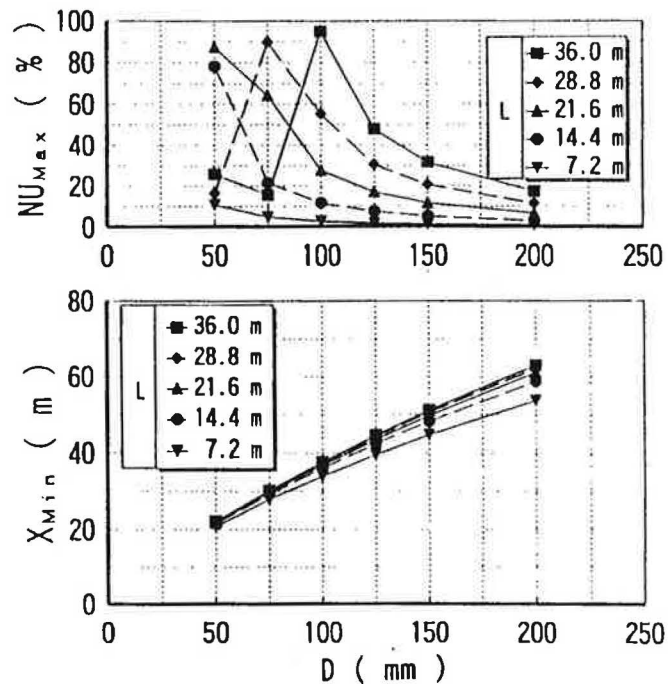


Fig. 3 Relation between  $NU_{Max}$  and  $X_{min}$  at various chamber heights. ( $d = 200$ ,  $Q = 30$ )

In general, the effective aperture of a diffuser outlet varies with the diameter, but we here take all apertures to be 0.4.<sup>7)</sup> In consideration of possibility of rupture of the caulking in floor seams, the upper limit to chamber pressurization was set at 50 Pa.<sup>8)</sup>

Figure 3 shows an example of analysis of the maximum non-uniformity resulting when the diffuser outlet resistance is not adjusted using filters. When  $X_{min} \geq L$ , the dynamic pressure near the neck area is high, and diffuser air flow rates are lower than the design values. As a result the maximum non-uniformity

diffuser air velocity appears in the neck area. And, the lower the chamber height, the greater the irregularity. On the other hand, when  $0 < X.i. < L$  the lionuniformity is maximum at the position of occurrence of the pressure **minimum**. When the position of occurrence of **minimum** press is exceeded the lionuniformity declines, and then increases once again.

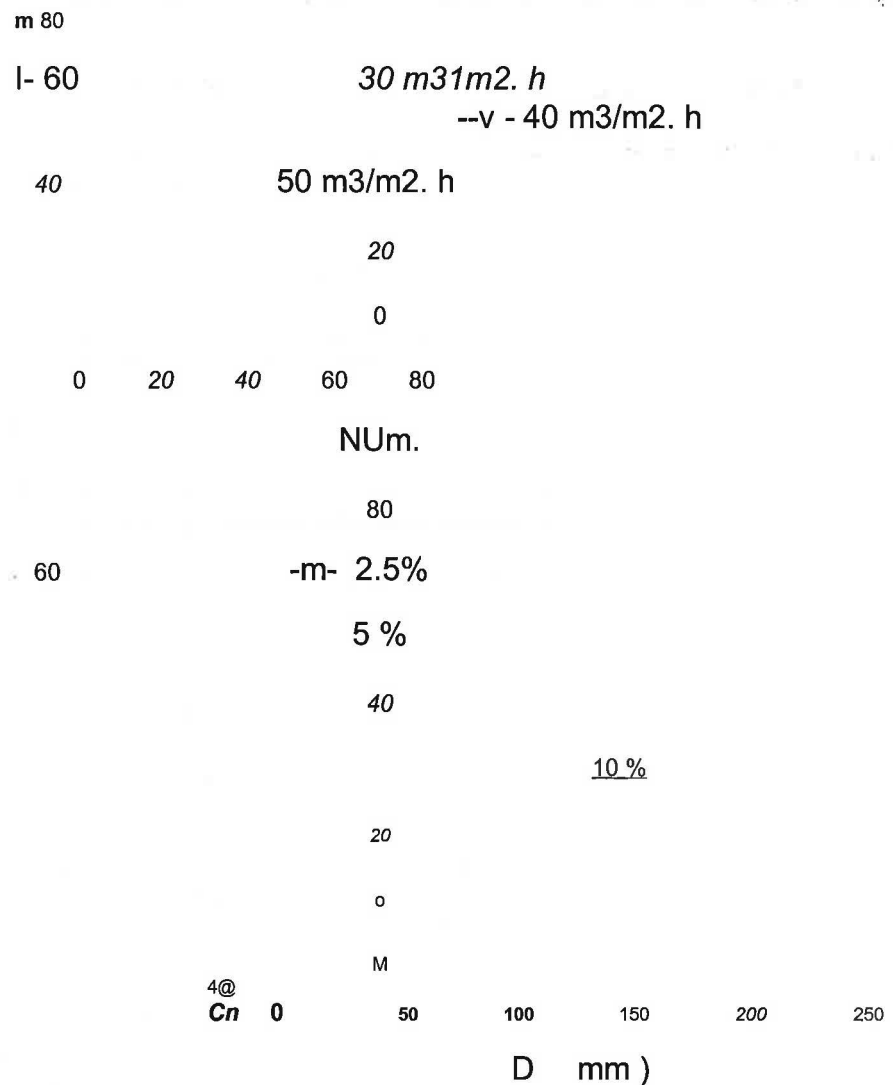


Fig. 4 Relation between necessary static pressure of a blower and chamber height, when NU, @, @, was controll  
 (Up: D = 100, d = 200, L = 36), (Down: d = 200, L = 36, Q = 30)

When filters with the same resistance value are installed on all diffusers, the blower static pressure required to obtain the target diffuser air velocity is as ill Figure 4. The greater the increase in unit air volume, the higher is the pressure required of the blower. Further, the longer the chamber, the higher the pressure that must be generated by the blower. When the chamber height is 50 mm or less, the static pressure required of the blower tends to rise rapidly. In view of the pressure limit imposed on the chamber and the rate of increase of the static pressure required of the blower, the lower limit to the floor height is thought to be 50 mm.

#### 4. Analysis of Sensitivity to Factors Governing Non-uniformity

As shown in Equation (23), the ratio of the pressure loss at the diffuser to the

dynamic pressure at the neck in the chamber can define as the diffuser resistance coefficient.2)

$$K = \frac{p_1 - p_2}{\rho U^2} + \frac{P_f}{\rho U^2} \quad (23)$$

Equation (23) can rewrite as follows from Equation (5) and Equation (19).

diffuser air velocity appears in the neck area. And, the lower the chamber height, the greater is the irregularity. On the other hand, when  $0 < X_{\min} < L$  the uniformity is maximum at the position of occurrence of the pressure minimum. When the position of occurrence of minimum pressure is exceeded the uniformity declines, and then increases once again.

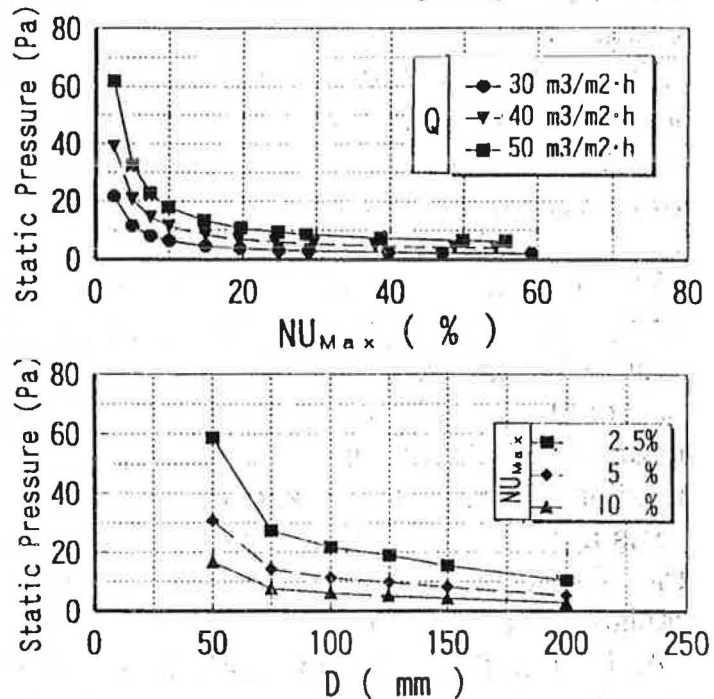


Fig. 4 Relation between necessary static pressure of a blower and chamber height, when  $NU_{Max}$  was controlled. ( Up:  $D = 100$ ,  $d = 200$ ,  $L = 36$ ), ( Down:  $d = 200$ ,  $L = 36$ ,  $Q = 30$ )

When filters with the same resistance value are installed on all diffuser blower static pressure required to obtain the target diffuser air velocity is shown in Figure 4. The greater the increase in unit air volume, the higher is the pressure required of the blower. Further, the longer the chamber, the higher the pressure that must be generated by the blower. When the chamber height is 100 mm or less, the static pressure required of the blower tends to rise rapidly. In view of the pressure limit imposed on the chamber and the rate of increase of the pressure required of the blower, the lower limit to the floor height is thought to be 50 mm.

#### 4. Analysis of Sensitivity to Factors Governing Non-uniformity

As shown in Equation (23), the ratio of the pressure loss at the diffuser to the dynamic pressure at the neck in the chamber can be defined as the diffuser resistance coefficient.<sup>2)</sup>

$$K = \{ \xi \cdot (\rho / 2) \cdot v^2 + P_f(v) \} / (\rho / 2) U^2 \quad \text{-----}$$

Equation (23) can be rewritten as follows from Equation (5) and Equation (19).



$$+ P f \alpha \cdot (p @, 2) \cdot V(2 @ - (8 \cdot K) 2$$

$$+ P f \alpha \cdot (p @, 2) \cdot V(2 @ \cdot [(4 \cdot (r r \cdot R K) @ \cdot (D \cdot L) \cdot (p \cdot d) 2) 12 \cdot \cdot \cdot \cdot (24)$$

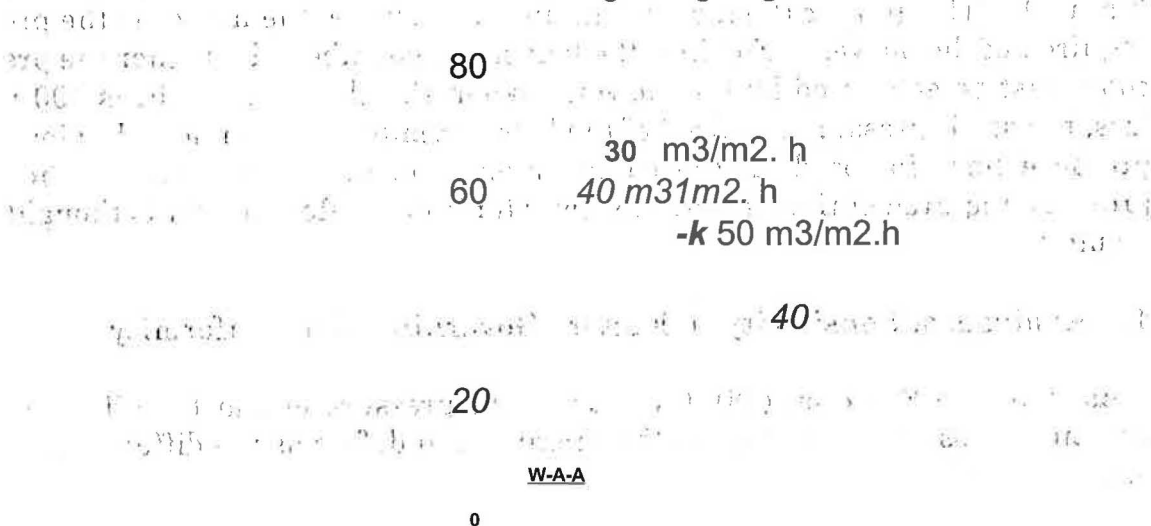
As Equation (24) indicates, the diffuser resistance coefficient is unrelated to the air volume or to the chamber width. Factors governing the diffuser

resistance coefficient include the chamber height, chamber length, diffuser outlet pitch and diameter, effective aperture, and diffuser filter resistance. Of these, the factors to which the resistance coefficient is most sensitive are the diffuser pitch and diameter.

The effect of factors governing the diffuser resistance coefficient on air flow, irregularity was studied. Filters were used to regulate the non-uniformity of the diffuser air flow; the relation between the maximum non-uniformity and the reciprocal of the diffuser resistance coefficient for various unit air volumes appears in Figure 5.

The chamber height tends to have a different effect at 75 mm and less compared with heights of 100 mm and above. This is because, as indicated in Figure 3, the minimum pressure position occurs within the chamber when the chamber height is 80 mm or less; the pressure distribution within the chamber changes at this height. If we suppose that for  $K > 1$  there is a proportional relation between the maximum non-uniformity and the reciprocal of the diffuser resistance coefficient, then the factors governing the maximum non-uniformity of the diffuser air velocity will be identical to the factors comprising the diffuser resistance coefficient.

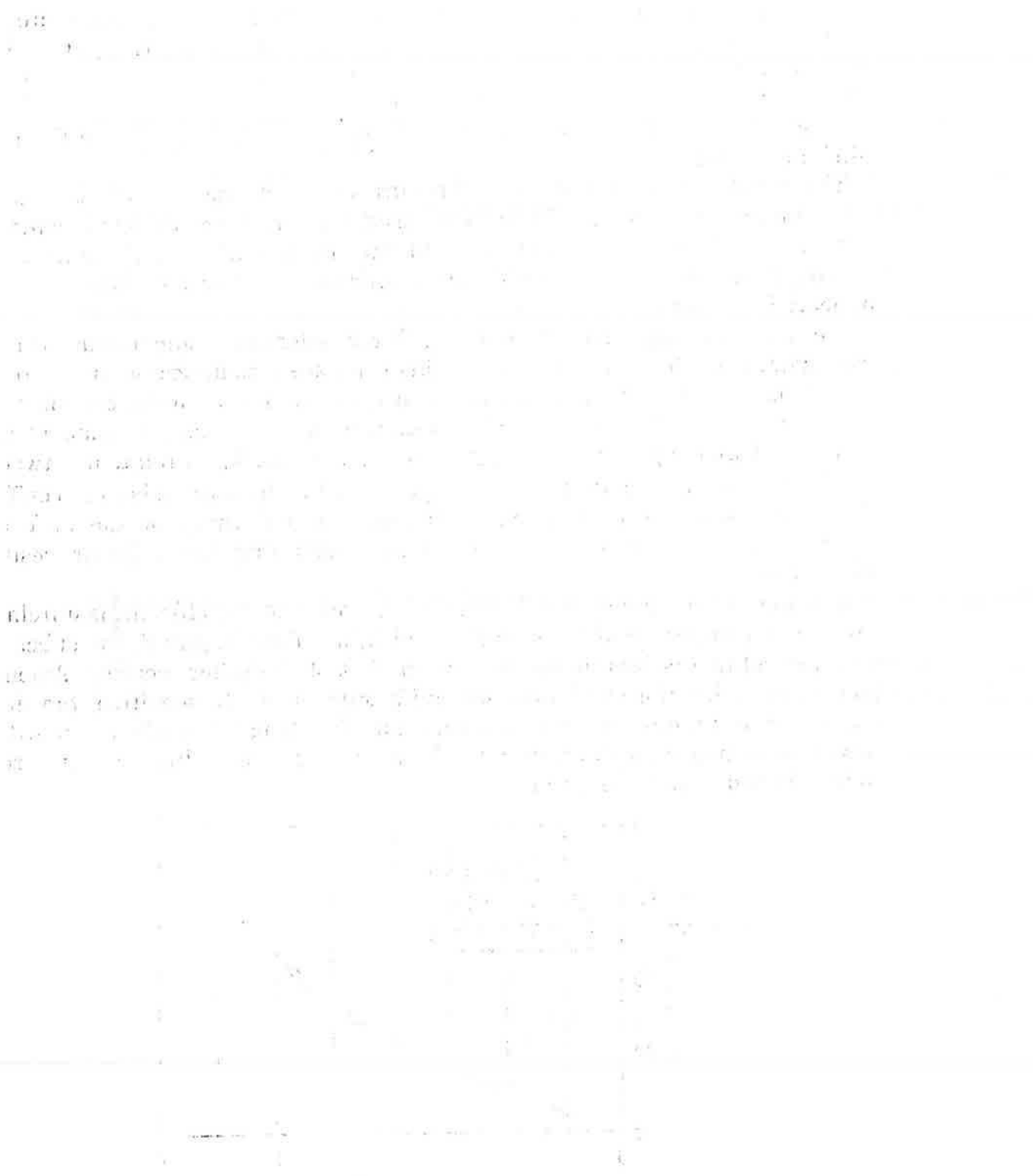
As indicated by Equation (24), the diffuser resistance coefficient is unrelated to the unit air volume and the chamber width; but from Figure 5, the effect of the unit air volume is less pronounced than that of the other factors. Among the factors to which the maximum non-uniformity is highly sensitive, the diffuser outlet diameter, effective aperture and chamber length are given quantities at design time; hence the diffuser pitch, chamber height, and filter resistance remain to be selected during designing.



W-A-A

0

Fig. 5 Relation between  $NU_{rj}$  and  $K^{-1}$  at various unit air volumes.  
 (D = 100, d = 200, L = 36)



$$\begin{aligned}
 K &= \{ \xi_0 + Pr_0 / (\rho / 2) / v_0^2 \} \cdot (\beta / \kappa)^2 \\
 &= \{ \xi_0 + Pr_0 / (\rho / 2) / v_0^2 \} \cdot \{ 4 / (\pi \cdot RK) \} \cdot (D / L) \cdot (p / d)^2
 \end{aligned}$$

As Equation (24) indicates, the diffuser resistance coefficient is unrelated unit air volume or to the chamber width. Factors governing the diffuser resistance coefficient include the chamber height, chamber length, diffuser pitch and diameter, effective aperture, and diffuser filter resistance. Of the factors to which the resistance coefficient is most sensitive are the diffuser pitch and diameter.

The effect of factors governing the diffuser resistance coefficient on maximum non-uniformity was studied. Filters were used to regulate the non-uniformity of diffuser air flow; the relation between the maximum non-uniformity and the reciprocal of the diffuser resistance coefficient for various unit air volumes appears in Figure 5.

The chamber height tends to have a different effect at 75 mm and less compared with heights of 100 mm and above. This is because, as indicated in Figure 1, the minimum pressure position occurs within the chamber when the chamber height is 80 mm or less; the pressure distribution within the chamber changes with height. If we suppose that for  $K \geq 1$  there is a proportional relation between maximum non-uniformity and the reciprocal of the diffuser resistance coefficient, then the factors governing the maximum non-uniformity of the diffuser air flow will be identical to the factors comprising the diffuser resistance coefficient.

As indicated by Equation (24), the diffuser resistance coefficient is unrelated to the unit air volume and the chamber width; but from Figure 5, the effect of unit air volume is less pronounced than that of the other factors. Among the factors to which the maximum non-uniformity is highly sensitive, the diffuser outlet diameter, effective aperture and chamber length are given quantitative design time; hence the diffuser pitch, chamber height, and filter resistance are to be selected during designing.

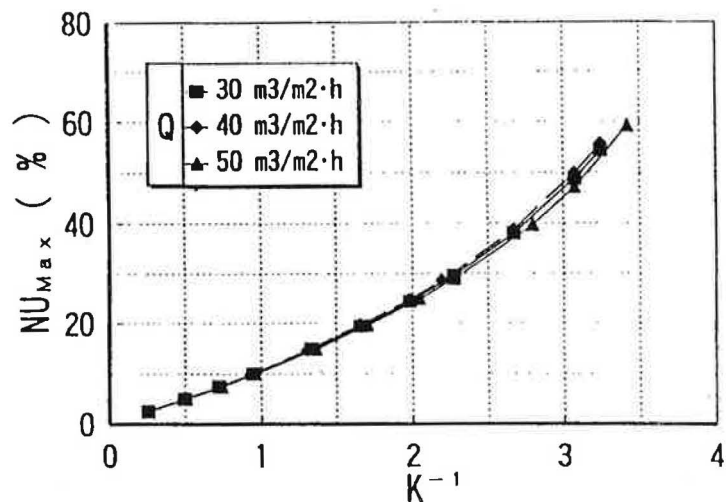


Fig. 5 Relation between  $NU_{Max}$  and  $K^{-1}$  at various unit air volumes. ( $D = 100$ ,  $d = 200$ ,  $L = 36$ )

If this proportional relation is used for  $K_{\theta} \rightarrow 1$ , then by specifying the maximum non-uniformity it becomes easy to choose a diffuser pitch, chamber height, and filter resistance values to adjust the non-uniformity in the air velocity profile.

### 5. Experimental Validation of Analytical Model

Using a scale model of the air supply chamber, the validity of the analytical model for determining non-uniformity in diffuser air velocity profiles was studied. 5.1 Experimental Apparatus and Experimental Conditions

Due to constraints on the size of the site for experiments, the validity of the analytical model was examined using a 1: 5 size scale model of the air supply chamber. The similarity of air flow in an actual system and in the scale model depends on agreement of the respective Reynolds numbers.

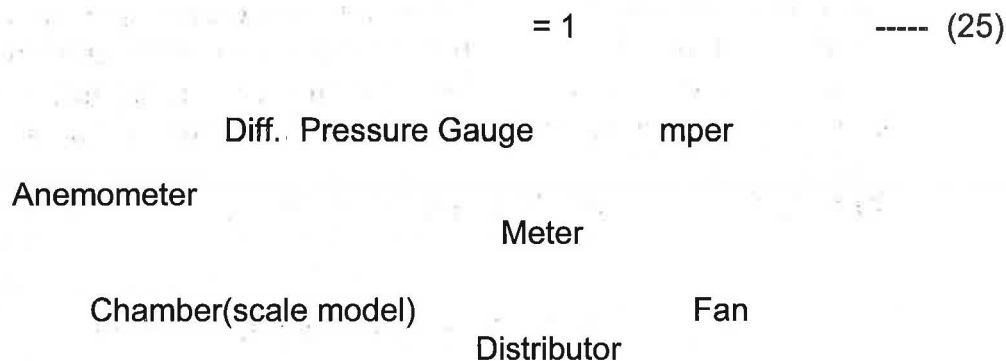


Fig. 6 Schematic diagram of experimental apparatus for scale model test.

However, the air flow velocities and pressures in a 1: 5 scale model are increased to 5 times and 25 times their values respectively in an actual system, which is not practical from the standpoint of chamber pressure resistance. The air flow is isothermal, and the Reynolds number at actual diffuser outlets is on the order of 10,000. In other words, because the air flow is well-developed turbulent flow, the conditions for self-similar flow obtain. The average Reynolds number for diffuser air flow in the model is of order 5,000, so that self-similar flow conditions obtain here as well. Hence the similarity conditions are relaxed, and for the model air flow a scale of unity was adopted.9)

Figure 6 is a schematic diagram of the model apparatus; the conditions of the model experiments appear in Table 2. The diameter of the model diffuser outlets was set at 20 mm, in consideration of an effective aperture of 0.4. After confirming that there were no leaks at Joints and points of connection with perforated plates in the model, an Annubar Werenial-pressure flow meter was used to measure the supplied air flow. Pressure differences were measured using a Benz manometer with a precision of  $\pm 1$  Pa. Air flow velocities were measured

If this proportional relation is used for  $K \geq 1$ , then by specifying the maximum non-uniformity it becomes easy to choose a diffuser pitch, chamber height, filter resistance values to adjust the non-uniformity in the air velocity profile.

## 5. Experimental Validation of Analytical Model

Using a scale model of the air supply chamber, the validity of the analytical model for determining non-uniformity in diffuser air velocity profiles was studied.

### 5.1 Experimental Apparatus and Experimental Conditions

Due to constraints on the size of the site for experiments, the validity of the analytical model was examined using a 1:5 size scale model of the air supply chamber. The similarity of air flow in an actual system and in the scale model depends on agreement of the respective Reynolds numbers.

$$(Re/Re_M) = (d \cdot v / \nu) / (d_M \cdot v_M / \nu) = 1$$

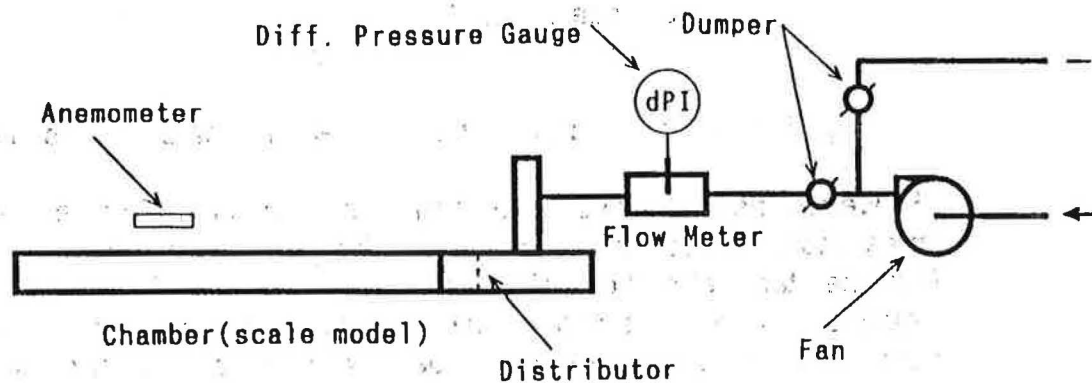


Fig. 6 Schematic diagram of experimental apparatus for scale model test

However, the air flow velocities and pressures in a 1:5 scale model are increased to 5 times and 25 times their values respectively in an actual system, which is not practical from the standpoint of chamber pressure resistance. The air flow is isothermal, and the Reynolds number at actual diffuser outlets is on the order of 10,000. In other words, because the air flow is well-developed turbulent flow conditions for self-similar flow obtain. The average Reynolds number for diffuser air flow in the model is of order 5,000, so that self-similar flow conditions obtain here as well. Hence the similarity conditions are relaxed, and for the model a scale of unity was adopted.<sup>9)</sup>

Figure 6 is a schematic diagram of the model apparatus; the conditions of model experiments appear in Table 2. The diameter of the model diffuser outlet was set at 20 mm, in consideration of an effective aperture of 0.4. To confirm that there were no leaks at joints and points of connection, perforated plates in the model, an Annubar differential-pressure flow meter was used to measure the supplied air flow. Pressure differences were measured with a Benz manometer with a precision of  $\pm 1$  Pa. Air flow velocities were measured

using multiple point hot-wire anemometers (KANOMAX model 6240). Measurement error over the measurement range determined using a wind tunnel for calibration were within m/s.

Table 2. Dimensions of experimental equipment and conditions at 1:5 scale.

Physical Parameter	Symbol	Unit	Quantities(real scale)	
width of chamber	WM	m	1.2 (6.0)	
diameter of diffuser	d,	mm	20 (200)	
effective opening ratio	RG		1	(0.4)
height of chamber	L		15(75)	30(150)
length of chamber	LM	m	2(10)	3 (15) 4 (20)
unit supplied air volume	QM	m <sup>3</sup> /ml.h	30	50
pitch of diffuser	PM	mm	400	300

Perforated plates were installed near the chamber neck, and by rectifying the supplied air, velocity component in the chamber width direction was eliminated in so far as possible. The velocity distribution in the chamber width direction was measured near the neck, and straightening effect of the perforated plates was confirmed. Non-uniformity in the air velocity profile in the chamber length direction were computed from the air flow velocities measured along the center line of the chamber.

#### 5.2 Comparison of Analysis and Experimental Results

The air flow velocity immediately above diffuser outlets is made unstable by the inductive effect. Air flow velocities were measured at positions at which

stable air flow measurement was possible, namely above the central line through the diffuser outlets, but removed a distance of 10 mm from a diffuser outlet plane. However, because of inductive effect of jet flow, the measured result differs from the true value of the air velocity. Therefore, we took the air velocity per diffuser as computed from the supplied air flow to be design air velocity, and computed correction coefficients for measurement positions from ratio of the average of the measured diffuser air velocities to the design air velocities; using these, the measured air velocities were converted into air velocities directly above the diffuser outlet using the following equation.

[Air Velocity Directly above Diffuser]

$$= [\text{Measured Air Velocity}] \cdot [\text{Measurement Position Correction Factor}] \quad \text{--- (26)}$$

Because calculated values include a measurement error of  $\pm 0.3$  m/s, measurement position correction factors were similarly used for conversion into measurement errors directly above diffusers.

The velocity distribution in the chamber width direction at the neck appears in Figure 7. The air flow velocities were computed as averages of five measurements at each of the measurement positions. Due to the straightening effect of the perforated plates, within the range of the experimental conditions,

using multiple point hot-wire anemometers (KANOMAX model Measurement errors over the measurement range determined using a wind for calibration were within  $\pm 0.3$  m/s.

Table 2. Dimensions of experimental equipment and conditions at 1:5 s

Physical Parameter	Symbol	Unit	Quantities(real scale)	
width of chamber	$W_M$	m	1.2 (6.0)	
diameter of diffuser	$d_M$	mm	20 (200)	
effective opening ratio	$RK_M$	-	1 (0.4)	
height of chamber	$D_M$	mm	15(75)	30(150)
length of chamber	$L_M$	m	2(10)	3 (15) 4 (20)
unit supplied air volume	$Q_M$	$m^3/m^2 \cdot h$	30	50
pitch of diffuser	$P_M$	mm	400	300

Perforated plates were installed near the chamber neck, and by rectifying supplied air, the velocity component in the chamber width direction eliminated in so far as possible. The air velocity distribution in the chamber width direction was measured near the neck, and the straightening effect of perforated plates was confirmed. Non-uniformity in the air velocity profile in chamber length direction were computed from the air flow velocities measured along the center line of the chamber.

### 5.2 Comparison of Analysis and Experimental Results

The air flow velocity immediately above diffuser outlets is made unstable by inductive effect of jet. Air flow velocities were measured at positions at which stable air flow measurement was possible, namely above the central line through the diffuser outlets, but removed a distance of 10 mm from a diffuser outlet. However, because of the inductive effect of jet flow, the measured result differed from the true value of the air velocity. Therefore, we took the air velocity directly above diffuser as computed from the supplied air flow to be the design air velocity and computed correction coefficients for measurement positions from the ratio of average of the measured diffuser air velocities to the design air velocities; with these, the measured air velocities were converted into air velocities directly above the diffuser outlet using the following equation.

$$[\text{Air Velocity Directly above Diffuser}] = [\text{Measured Air Velocity}] / [\text{Measurement Position Correction Factor}]$$

Because calculated values include a measurement error of  $\pm 0.3$  m/s, measurement position correction factors were similarly used for conversion of measurement errors directly above diffusers.

The velocity distribution in the chamber width direction at the neck appeared in Figure 7. The air flow velocities were computed as averages of measurements at each of the measurement positions. Due to the straightening effect of the perforated plates, within the range of the experimental conditions

deviations from average values were in all cases within 4- 10 %. This confirmed validity of Assumption (4).

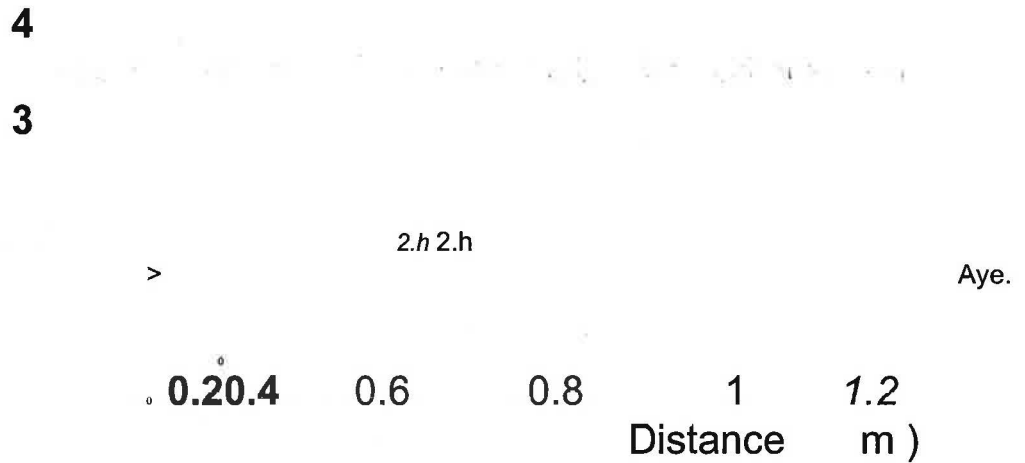


Fig. 7 Vertical diffuser air velocity profile on the neck in the scale and the effect of a distributor by perforated panels. (1)m = 30, Lm = 4, W-, @i = 1.2)

The experimental results as converted into air velocities directly above diffusers, and air velocity profile in the chamber length direction as computed using the analytical model appear in Figure 8. The experimental conditions were in all cases such that  $(D.W., T > 1)$ , satisfying this condition on the validity of the analytical model.

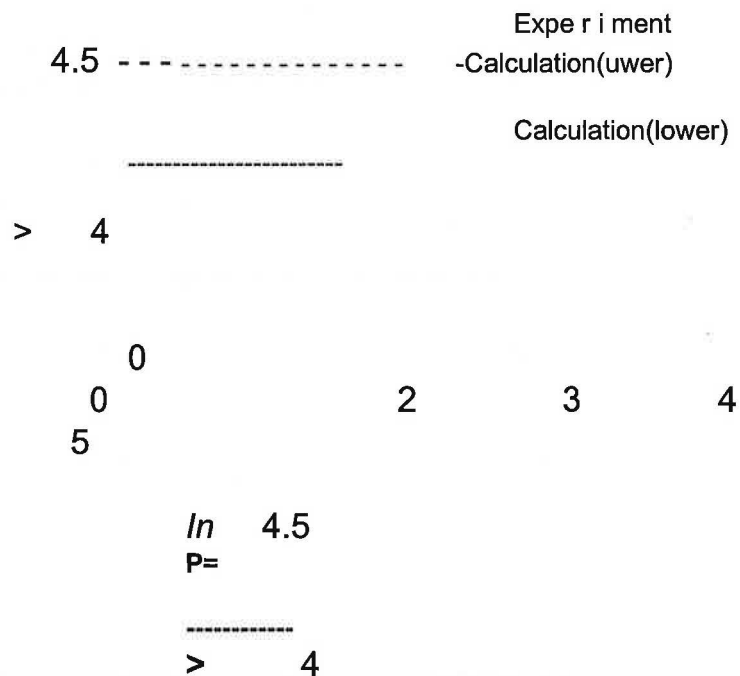


Fig. 8 Comparison with the experiment and calculation on longitudinal diffuser

01 2 3 4  
Distance (m)



air velocity profile from  
the neck to the bulkhead at  $D_m = 30$ ,  $Q_{xi} = 30$ . (up:  $L_m = 2$ , down: L  
4)

The experimental and analytical results reveal an increase in air velocity due to

deviations from average values were in all cases within  $\pm 10\%$ . This confirms the validity of Assumption (4).

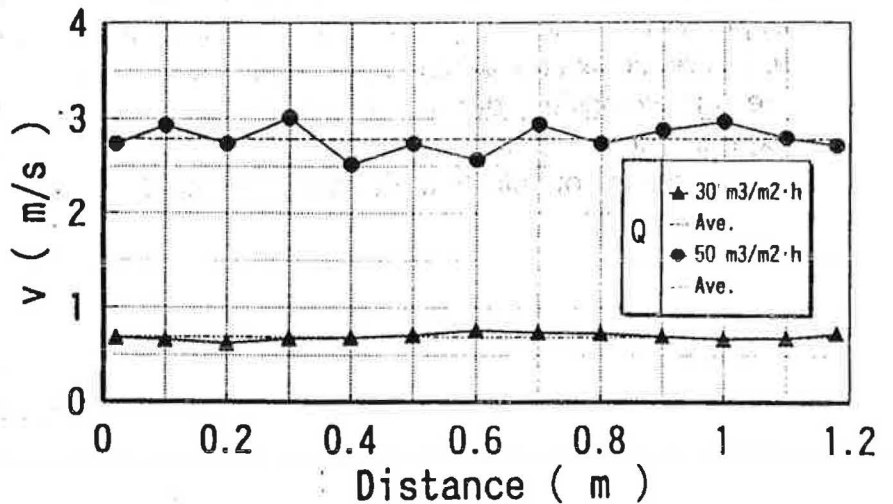


Fig. 7 Vertical diffuser air velocity profile on the neck in the scale and the effect as a distributor by perforated panels. ( $D_M = 30, L_M = 4, W_M = 1$ )

The experimental results as converted into air velocities directly above diffusers and the air velocity profile in the chamber length direction as computed using an analytical model, appear in Figure 8. The experimental conditions were cases such that  $(D \cdot W / \Sigma s) > 1$ , satisfying this condition on the validity of the analytical model.

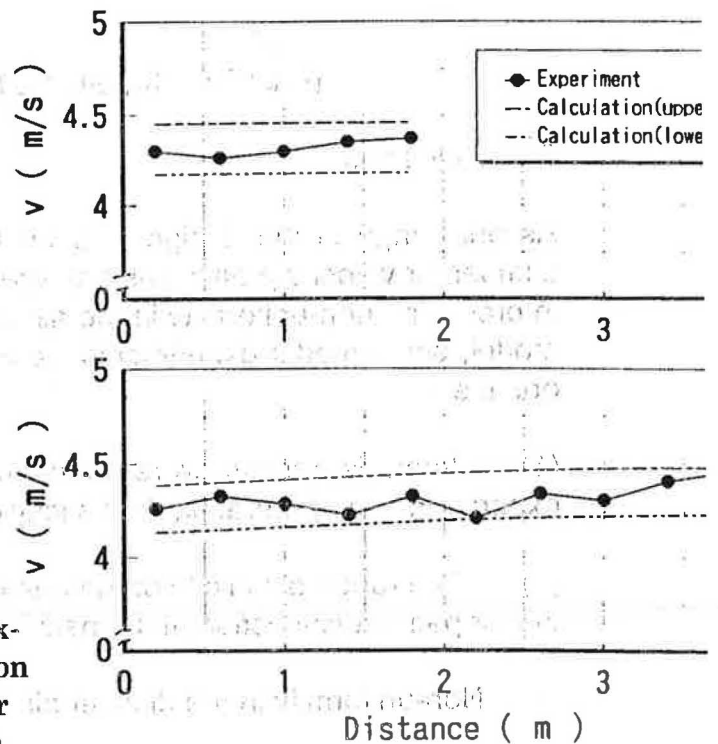


Fig. 8 Comparison with the experiment and calculation on longitudinal diffuser air velocity profile from the neck to the bulkhead at  $D_M = 30, Q_M = 30$ . (up:  $L_M = 2$ , down:  $L_M = 4$ )

The experimental and analytical results reveal an increase in air velocity d

reacquisition of static pressure from the neck area to the bulkhead. The range of measurement error was set for analysis results, but in any event the results are within the range of measurement error, thus confirming the validity of the analytical model. In order to verify experimentally the conditions for validity of the analytical model, the chamber height of the model was changed from 15 to 10 mm, the pitch of the diffusers was reduced from 300 to 200 mm, and air velocities were measured under these new conditions which deviated from the range for which the analytical model applies. Experimental and analytical results obtained for  $(D, W, \tau) = 0.319$  appear in Figure 9. No reacquisition of static pressure is observed from the neck to the bulkhead, and the air velocities decline uniformly. Moreover, the air velocity profiles of the experimental and analytical results are reversed. These experiments thus confirmed the conditions of validity of the analytical model.

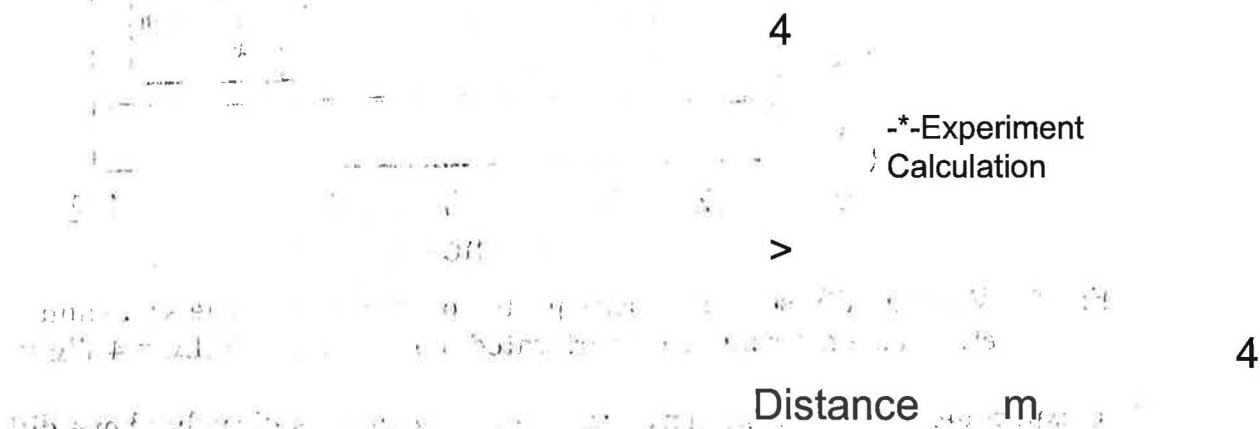


Fig. 9 Comparison with the experiment and the calculation result on longitudinal diffuser air velocity profile at  $(D, W, \tau) = 0.319$ .

91  
 $(D, \tau = 10, \text{pm} = 200, L_m = 4, Q_m = 48, W_m = 1.2)$

## 6. Conclusions

As one stage in the design of a pressurized under-floor air-conditioning system, the diffuser air velocity profile was analyzed, and an analytical model was proposed for use in predicting non-uniformity in the air velocity profile. In order to verify the validity of the model, scale model experiments were performed, and the following conclusions were obtained.

- (1) Analysis results were in good coincidence with values obtained in model experiments, corroborating the validity of the analytical model.
- (2) The range of validity of the analytical model is that range of parameters for which the air path cross-section at the neck is greater than the total area of all diffuser outlets.
- (3) Non-uniformity in the diffuser air velocity profile for chamber heights of 100

reacquisition of static pressure from the neck area to the bulkhead. The measurement error was set for analysis results, but in any event the results were within the range of measurement error, thus confirming the validity of the analytical model. In order to verify experimentally the conditions for validity of the analytical model, the chamber height of the model was changed from 150 mm, the pitch of the diffusers was reduced from 300 to 200 mm, and air velocities were measured under these new conditions which deviated from the range in which the analytical model applies. Experimental and analytical results obtained for  $(D \cdot W / \Sigma s) = 0.319$  appear in Figure 9. No reacquisition of static pressure is observed from the neck to the bulkhead, and the air velocities do not become uniform. Moreover, the air velocity profiles of the experimental and analytical results are reversed. These experiments thus confirmed the conditions of validity of the analytical model.

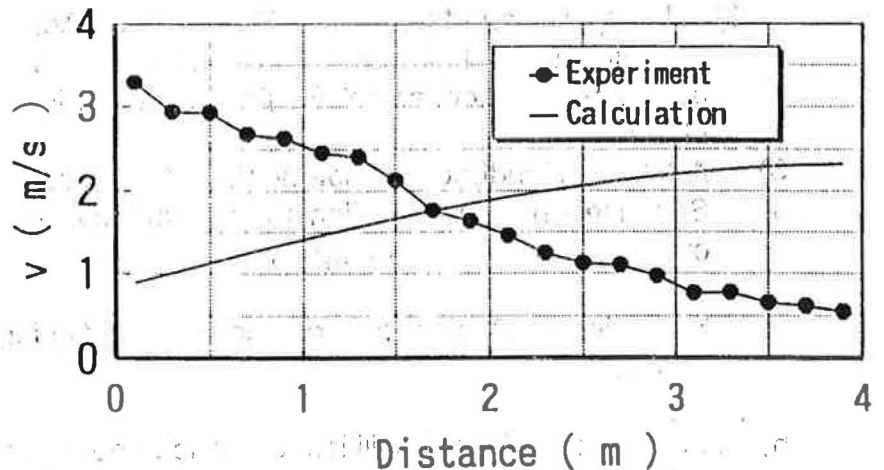


Fig. 9 Comparison with the experiment and the calculation result on longitudinal diffuser air velocity profile at  $(D \cdot W / \Sigma s) = 0.319$  ( $D_M = 10$ ,  $p_M = 200$ ,  $L_M = 4$ ,  $Q_M = 48$ ,  $W_M = 1.2$ )

## 6. Conclusions

As one stage in the design of a pressurized under-floor air-conditioning system, the diffuser air velocity profile was analyzed, and an analytical model proposed for use in predicting non-uniformity in the air velocity profile. In order to verify the validity of the model, scale model experiments were performed and the following conclusions were obtained.

- (1) Analysis results were in good coincidence with values obtained in experiments, corroborating the validity of the analytical model.
- (2) The range of validity of the analytical model is that range of parameter values for which the air path cross-section at the neck is greater than the total area of diffuser outlets.
- (3) Non-uniformity in the diffuser air velocity profile for chamber heights of

mm to 300 mm, for which there are performance records for numerous pressurized under-floor air-conditioning systems, were approximately 10 % or less. The lower limit for the chamber height was 50 mm.

(4) As a method of regulating non-uniformity in diffuser air velocity emerging as the floor height is lowered, installation of filters with same resistance value on all diffuser outlets is effective. This method is more energy-efficient as a means of regulating non-uniformity in air flow velocity than is the conventional method of installing dampers at floor diffusers and using the damper apertures to regulate air flow.

(5) It was shown that for diffuser resistance coefficients of unity or greater, the resistance coefficient is proportionally related to the maximum non-uniformity of the diffuser air velocity. Using this relation, the pressurized diffuser pitch, chamber height and filter resistance values can easily be chosen so as to adjust non-uniformity in the air flow velocity profile.

#### References

- 1) H. Hayama and M. Alikami: Report of the Annual Meeting of the Architectural Institute of Japan (1990), 1203.
- 2) Japan Soc. Mechanical Engineers, ed.: Fluid Resistance of Pipes and Ducts (1991), 96.
- 3) ASHRAE Handbook: Fundamentals (1981), 33.7 and 33.27.
- 4) Soc. Heating, Air Conditioning and Sanitary Engineering of Japan, ed.: Handbook of Heating, Air Conditioning and Sanitation, 11th ed. (1989), 11-305.
- 5) M. Ishiura: Design of Architectural Ventilation (1969), 283, Asakura Shoten publication.
- 6) Y. Hiruma: Ancillary Facilities for Roads and Tunnels (1966), 88, Rikougaku Tosho publication.
- 7) H. Fujita, T. Hori, S. Hachisuka and T. Nishio: Report of the Annual Meeting of the Architectural Institute of Japan (1989), 1181.
- 8) M. Hirayama, T. Nishio, T. Hori, E. Komlya and S. Tanabe: Trans. Soc. Heating, Air Conditioning and Sanitary Engineers of Japan (1991), 173.
- 9) I. Emori: Theory and Application of Model Experiments (1985), 37, Gihoudou publication.

#### Symbols

D	Height of chamber [ m ]
DE	Equivalent diameter of chamber [ m ]
d	Diameter of diffuser outlet [ m ]
K	Resistance coefficient of diffuser
L	Length of chamber [ m ]

m Number of diffusers in length direction

<b>N</b>	Number of diffusers in width direction	
<b>p</b>	Pressure [ Pa ]	
<b>Pf (v)</b>	Filter resistance [ Pa ]	
<b>p</b>	Pitch of diffuser outlet	
<b>Q</b>	Unit air volume [M <sup>3</sup> ,M <sup>2</sup> .h]	
<b>RK</b>	Effective aperture of diffuser outlet	
<b>8</b>	Area of diffuser [ M <sup>2</sup> ]	
<b>u</b>	Air speed at neck [ m,,s ]	
<b>NU</b>	Non-uniformity in supplied air velocity profile	%
<b>NUm..</b>	Maximum non-uniformity [ % ]	
<b>v</b>	Diffused air velocity [ m,,s ]	
<b>W</b>	Width of Chamber [ m ]	
<b>Xrnin</b>	Position of appearance of minimum pressure	m
<b>16</b>	: Diffuser aperture ratio [ - ]	
<b>K</b>	: Ratio of air path cross-section to floor area	
<b>A</b>	: Tube friction coefficient [ - ]	
<b>0</b>	: Outlet orifice loss coefficient	
<b>2</b>	: Branch loss coefficient [ - ]	
<b>v</b>	Air dynamic viscosity coefficient [M <sup>2</sup> ,,S]	
<b>p</b>	Air density [kg,-IM <sup>3</sup> ]	

#### Subscripts

<b>1</b>	Neck
<b>m</b>	Scale model

- m nth number of diffuser outlet at which minimum pressure appears
- nth number of diffuser outlet
- Bulkhead
- Room
- Arbitrary distance

$M$	: Number of diffusers in length direction [ - ]
$N$	: Number of diffusers in width direction [ - ]
$P$	: Pressure [ Pa ]
$P_f(v)$	: Filter resistance [ Pa ]
$p$	: Pitch of diffuser outlet [ m ]
$Q$	: Unit air volume [ m <sup>3</sup> /m <sup>2</sup> ·h ]
$RK$	: Effective aperture of diffuser outlet [ - ]
$s$	: Area of diffuser [ m <sup>2</sup> ]
$U$	: Air speed at neck [ m/s ]
$NU$	: Non-uniformity in supplied air velocity profile [ % ]
$NU_{Max}$	: Maximum non-uniformity [ % ]
$v$	: Diffused air velocity [ m/s ]
$w$	: Width of Chamber [ m ]
$X_{min}$	: Position of appearance of minimum pressure [ m ]
$\beta$	: Diffuser aperture ratio [ - ]
$\kappa$	: Ratio of air path cross-section to floor area [ - ]
$\lambda$	: Tube friction coefficient [ - ]
$\zeta_0$	: Outlet orifice loss coefficient [ - ]
$\zeta_2$	: Branch loss coefficient [ - ]
$\nu$	: Air dynamic viscosity coefficient [ m <sup>2</sup> /s ]
$\rho$	: Air density [ kg/m <sup>3</sup> ]

### Subscripts

$l$	: Neck
$M$	: Scale model
$m$	: mth number of diffuser outlet at which minimum pressure appear
$n$	: nth number of diffuser outlet
$0$	: Bulkhead
$r$	: Room
$x$	: Arbitrary distance